THE JOURNAL OF PHYSICAL CHEMISTRY C

ARTICLE

pubs.acs.org/JPCC

Does Bridging Geometry Influence Interfacial Electron Transfer Dynamics? Case of the Enediol-TiO_2 System

Sreejith Kaniyankandy,[§,†] Sachin Rawalekar,[†] Anik Sen,[‡] Bishwajit Ganguly,[*,‡] and Hirendra N. Ghosh[*,†]

[†]Radiation and Photochemistry Division, Bhabha Atomic Research Centre, Mumbai 400085, India

[‡]Analytical Science Discipline, Central Salt and Marine Chemicals Research Institute (CSIR), Bhavnagar, Gujarat 364002, India

Supporting Information

ABSTRACT: We have employed femtosecond transient absorption spectroscopy in enediol-TiO_2 systems (catechol, resorcinol, and quinol) to understand localized vs delocalized interfacial electron transfer dynamics in dye-nanoparticle systems. Optical absorption studies confirmed the formation of a charge transfer (CT) complex between the enediols and TiO_2 nanoparticles. CT interaction between enediols and TiO_2 was found to be decreased from catechol to resorcinol to quinol. The decrease in interaction strength from catechol to quinol was explained on the basis of a reduced overlap between the HOMO localized on the enediol and the conduction band of TiO_2. Femtosecond transient absorption studies confirmed an ultrafast electron injection (<50 fs) into the conduction band of TiO_2 in all enediol-TiO_2 systems. Interestingly back electron transfer (BET), which follows multiexponential dynamics, is faster in the catechol-TiO_2 system as compared to the other two enediol-TiO_2 systems. As we increase the distance between the bridging ligand from catechol to quinol, we find that decay time increases proving the influence of bridging distance between enediols and TiO_2. Our theoretical studies indicate an increase in the delocalization of the injected electron over several Ti atoms as the distance between the bridge linkers increases. Analysis of BET results in the framework of the Marcus theory indicated a significant influence of electronic coupling on BET in the enediol-TiO_2 systems.

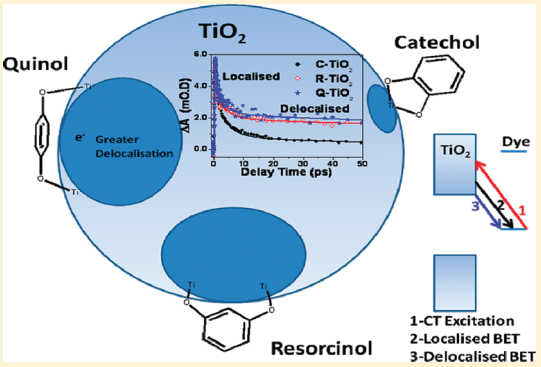

1. INTRODUCTION

Interfacial electron transfer forms the basis of several physical and biological processes.[1−4] Interest in this field has been growing due to their role in diverse applications like photocatalysis, photovoltaics, molecular electronics, etc.[5,6] The field of dye-sensitized solar cells has grown immensely from the knowledge gained by studies of electron transfer at interfaces. Electron transfer at semiconductor-dye interfaces forms the basis of dye-sensitized solar cell applications.[2] Since the electron transfer is aided by binding groups on the dyes, study of its influence has been a starting point of several investigations.[7,8] Various groups have demonstrated the influence of binding groups on the injection rate, yield, etc.[7] Furthermore, studies on the injection and back electron rates have enabled the understanding and refining of the materials for optimizing device performance. Among the binding groups, strong binding components like catechol, iso-nicotinic acid, etc.[9−12] enable a very high injection yield. However, it has been well reported in the literature that in such strong binding cases, a strong electronic coupling itself facilitates a faster back electron transfer (BET), which is detrimental for photovoltaic devices.[13,14] In the present investigation, we aim to study the prototypical strong binding components by comparing the charge transfer (CT) dynamics in catechol-, resorcinol-, and quinol-sensitized (referred to as enediols) TiO_2 nanoparticles. Here, the position between two hydroxyl groups changes the coupling between enediols and TiO_2 nanoparticles. In these cases, the positioning of the two hydroxyl groups changes due to the molecular structure itself; therefore, the binding of the enediol to the TiO_2 surface takes place by a bidentate binuclear arrangement. Here, the Ti involved in the binding could be the second, third, or fourth Ti from the first OH binding site depending on the position of the OH groups in the enediol. Since the HOMO and LUMO positions are more or less similar for these molecules,[15] the changes in the absorption spectrum on binding can be a clear evidence of the effect of the binding configuration of a strongly coupled charge transfer (CT) complex or relatively weaker CT complex. In view of the present investigation, we can expect localized CT for a stronger complex and delocalized CT in a relatively weaker complex. Previous studies on the catechol-TiO_2 system clearly showed a fast recombination with ∼80% of components decaying within 10 ps.[9,16] The fast BET process arises to be due to the recombination of an injected hot electron believed to be localized in the chelating site. Therefore, in the cases of resorcinol and quinol, the two Ti^{4+} ions involved in binding are positioned remote from each other; therefore, the electron is expected to delocalize over a larger area, which may lead to a

Received: July 24, 2011
Revised: November 10, 2011
Published: November 11, 2011

dx.doi.org/10.1021/jp207054f | J. Phys. Chem. C 2012, 116, 98–103

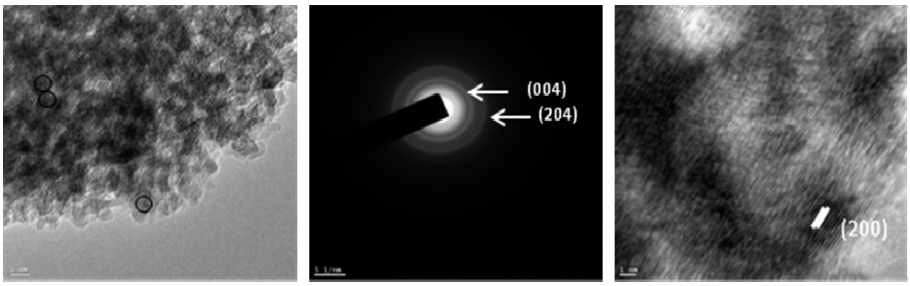

Figure 1. Transmission electron microscopy (high and low magnifications) and electron diffraction of TiO_2.

decrease in the localized electron recombination component. Additionally, this study also shows how subtle variation in the positioning of the binding groups governs the recombination dynamics. We attempt to study the influence of coupling of the linkers by carrying out sensitization of TiO_2 with these enediols and study the interfacial electron transfer dynamics by femtosecond transient absorption experiments.

2. EXPERIMENTAL SECTION

2.1. Femtosecond Transient Absorption Studies. The femtosecond tunable visible spectrometer has been developed based on a multipass amplified femtosecond Ti:sapphire laser system supplied by Thales, France.[17] The pulses of 20 fs duration and 4 nJ energy per pulse at 800 nm obtained from a self-mode-locked Ti:sapphire laser oscillator (Synergy 20, Femtolaser, Austria) were amplified in a regenerative and two-pass amplifier pumped by a 20 W DPSS laser (Jade) to generate 40 fs laser pulses of about 1.2 mJ energy at a repetition rate of 1 kHz. The 800 nm output pulse from the multipass amplifier is split into two parts to generate pump and probe pulses. In the present investigation, we have used frequency doubled 400 nm as the excitation sources. To generate pump pulses at 400 nm, one part of 800 nm with 200 μJ/pulse is the frequency doubled in BBO crystals. To generate visible probe pulses, about 3 μJ of the 800 nm beam is focused onto a 1.5 mm thick sapphire window. The intensity of the 800 nm beam is adjusted by iris size and ND filters to obtain a stable white light continuum in the 400 nm to over the 1000 nm region. The probe pulses are split into the signal and reference beams and are detected by two matched photodiodes with variable gain. We have kept the spot sizes of the pump beam and probe beam at the crossing point around 500 and 300 μm, respectively. The noise level of the white light is about ~0.5% with occasional spikes due to oscillator fluctuation. We have noticed that most laser noise is low-frequency noise and can be eliminated by comparing the adjacent probe laser pulses (pump blocked vs unblocked using a mechanical chopper). The typical noise in the measured absorbance change is about <0.3%. The instrument response function (IRF) for 400 nm excitation was obtained by fitting the rise time of the bleach of sodium salt of *meso*-tetrakis(4-sulfonatophenyl)porphyrin (TPPS) at 710 nm and found to be 120 fs. All solutions were circulated to avoid sample bleaching during the course of the experiment. The data analysis and fitting at individual wavelengths were carried out by the Lab-View program.

2.2. Synthesis of TiO_2 Nanoparticles. Synthesis was carried out by modifying a previously reported procedure.[18] Briefly, 0.3 g of titanium isopropoxide was added to 5 mL of ethylene glycol and 4 mL of an oleic acid mixture at room temperature.

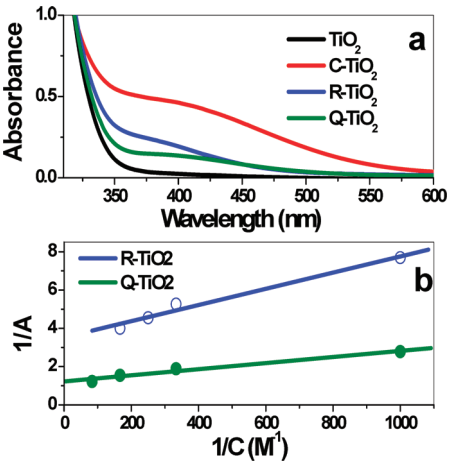

Figure 2. (a) UV−vis absorption spectrum of the catechol-TiO_2 (C-TiO_2), resorcinol-TiO_2 (R-TiO_2), and quinol-TiO_2 (Q-TiO_2) complexes. (b) Benesi−Hildebrand Plot for Q-TiO_2 and R-TiO_2 for different concentrations of the dye. Note: In panel b, C is the concentration of the dye, A is the absorbance, and the straight lines are the linear fits.

The above mixture was stirred for 30 min after which 20 mL of water was added under vigorous stirring. The above solution was heated to 100 °C under reflux conditions. The solution was precipitated by the addition of acetone. The precipitate was later cleaned by dissolving in toluene and again precipitating with 10% acetone (in methanol) at least 3 times. The powder was dried in ambient conditions and used for further studies. For UV−visible absorption and femtosecond transient studies, the particles were dissolved in chloroform.

2.3. Sensitization of TiO_2 Nanoparticles with Enediols. TiO_2 nanoparticles were dissolved in chloroform with a concentration of 4 g/L. To this solution, catechol, resorcinol, and quinol were added and allowed for sensitization for 4 h. The sensitized samples are hereby referred to as C-TiO_2, R-TiO_2, and Q-TiO_2 for catechol-, resorcinol-, and quinol-sensitized TiO_2, respectively.

3. RESULTS AND DISCUSSION

The transmission electron microscopy (TEM) studies (Figure 1) show the particle size to be ~3 nm with a fairly good size distribution. The electron diffraction taken over a large area shows sharp rings indicating the samples are crystalline. The rings can be assigned to different planes of the anatase phase of TiO_2.

The broad band centered in the blue region and extending toward the red region as shown in Figure 2a is a typical feature of enediol-TiO_2 systems. Enediols in the native state absorbs below

dx.doi.org/10.1021/jp207054f |J. Phys. Chem. C 2012, 116, 98–103

Table 1. Spectroscopic Parameters and Coupling Elements (H_{ab}) of Various Enediol-TiO_2 Nanoparticle Complexes

sample	ε_{max} (M^{-1} cm^{-1})	K_f (M^{-1})	H_{ab} (cm^{-1})
$(NH_4)_2Ti(Cat)_3$, (Cat = Catechol) [20]	10^4		
C-TiO_2	$\sim 10^3$	$\sim 10^3$	3125
R-TiO_2	31.4 (365 nm)	765.6	453.2
Q-TiO_2	10.9 (383 nm)	246.9	246.9

280 nm, which is attributed to the π(HOMO)−π^*(LUMO) transition. The formation of the new band extending from the UV to visible region has been previously assigned to the LMCT (ligand to metal charge transfer) transition from the π-orbital of the diol to the empty conduction band consisting of the d-orbital centered on Ti^{4+}.[16,19] Formation of the LMCT band indicates that the binding between the TiO_2 surface and the enediol is quite strong. To estimate the electronic coupling strength between enediol-TiO_2 systems, we have determined extinction coefficient of the CT complex from the Benesi−Hildebrand plot in Figure 2b (see also Supporting Information). The plot shows a straight line for resorcinol and quinol indicating that the binding is mainly by a single mode, which was previously assigned to a dissociative bridge binding.[20] The extinction coefficient obtained for the complexes is found to increase in the order $\varepsilon_{catechol} > \varepsilon_{resorcinol} > \varepsilon_{quinol}$. Since CT transition arises from the mixing of excited (CB of TiO_2) and ground states (HOMO of the Dye), the trends of the extinction coefficient indicates, as we increase the distance between the bridging ligands, that there is a decrease in overlap between the CB of TiO_2 and the HOMO of catechol.

In order to understand the strength of the electronic interaction between TiO_2 and enediols in the ground state, we have estimated the strength of electronic coupling H_{ab} by using the Mulliken[21] and Hush[22] equations. The approximate peak position and width of the CT bands were obtained by subtracting the TiO_2 absorption spectrum from the enediol-TiO_2 absorption spectrum and fitting the CT band with a Gaussian.

The electronic coupling parameter H_{ab} was calculated by the following formula:

$$H_{ab} = 2.06 \times 10^{-2} \frac{\bar{\nu}_{max} \times \varepsilon_{max} \times \Delta\bar{\nu}_{1/2}}{r_{ab}}$$

where $\bar{\nu}_{max}$ (reciprocal of the peak position of the CT band) is expressed in cm^{-1}, ε_{max} (extinction coefficient at the peak position) is in M^{-1} cm^{-1}, and $\Delta\bar{\nu}_{1/2}$ (fwhm of the CT band) is in cm^{-1}.

The above calculations show that electronic coupling varies as H_{ab} (catechol) ≫ H_{ab} (resorcinol) > H_{ab} (quinol) (see Table 1). It is necessary to find out if this decrement is due to the alignment of the benzene ring of the enediol with the respect to the surface of TiO_2. Catechol, which binds by adjacent OH groups, is expected to align in such a way that the benzene ring is normal to the nanoparticle surface. Similar geometry can be expected for resorcinol. However, in the case of quinol, the geometry is expected to be parallel to the surface as a perpendicular configuration, which might lead to significant steric hindrance. If we assume that the orientation of the π-ring with the TiO_2 surface is responsible for the reduction in H_{ab}, then we should observe a significant change in electronic interaction for resorcinol and quinol as the orientation changes from parallel to perpendicular, which is certainly not observed in the present investigation. Instead, we find a significant decrease in the coupling of the quinol-TiO_2 system as compared to the catechol-TiO_2 system. So, we can safely argue that the π-ring orientation with the nanoparticle surface is not the primary cause for a significant decrease in the electronic coupling matrix. This argument is also supported by the fact that the CT interaction that takes place between the TiO_2 surface and the enediols are mediated via the bridging groups rather than the benzene ring overlap. Therefore, the primary reason for the drastic reduction in H_{ab} could be due to the electronic structure of the excited state where the number of Ti involved in the linkage increases from catechol to quinol. In this situation, we can imagine that the degree of charge delocalization will be different in the enediol-TiO_2 systems as we move from the ortho (1,2) to the meta (1,3) to the para (1,4) enediol since H_{ab} is related to the wave function overlap between the ground state composed of π-orbitals localized on the benzene ring and conduction band consisting of d-orbitals of Ti^{4+}. So, it is expected that the spread of the electron cloud over several Ti, in the cases of resorcinol and quinol, may significantly decrease the oscillator strength of CT transitions. Interestingly, in steady-state absorption, we have observed a higher intensity of steady-state absorption for the catechol-TiO_2 CT complex as compared to the resorcinol/quinol-TiO_2 systems. In addition to that, this argument is well supported by literature studies, which indicate that in the case of $(NH_4)_2Ti(Cat)_3$, where the catechol molecule is bound to a single Ti^{4+}, the ε is an order of magnitude higher (10^4 M^{-1} cm^{-1})[18] compared to the catechol bound to TiO_2 ($\sim 10^3$ M^{-1} cm^{-1}) (Table 1). These arguments are suitably supported by theoretical studies as discussed below.

To examine the influence of bridging linkers on CT transitions, density functional calculations with GGA/PW91/DND have been performed using a titanium dioxide cluster $[Ti_8O_{32}]$.[23−30] The optimization of the complexed dyes with the TiO_2 surface was performed in gas phase, and single-point calculations were carried out in chloroform using the COSMO solvation model.[31−33] The binding of the dye with the TiO_2 cluster leads to the restructuring of the energy levels. The TiO_2 anatase {101} plane was constructed based on earlier reports for the interaction of catechol.[19,34] The primary effect of binding between the dye and TiO_2 is apparent in the contribution to the LUMO, which predominantly arises from the Ti-3d orbital. The DFT calculated frontier molecular orbital of the ligand complexed TiO_2 in chloroform is given in Figure 3a. The calculated frontier molecular orbitals for the interaction of catechol with the TiO_2 surface is similar to that obtained by Duncan and Prezhdo.[19] The energy gap between the FMOs for catechol with the TiO_2 surface is 1.38 eV (see Figure 3a), which increases in the case of resorcinol 1.67 eV (see Figure 3b). This difference presumably arises due to the different mode of binding of these two enediols with the TiO_2 surface. Quinol with 1,4-dihydroxy groups can have a similar effect in the CT transition as the bridging units are further away as compared to catechol and resorcinol. In the case of quinol, the oxygens of the diols are at an angle to the ring plane indicating significant distortions. This distortion arises due to the large O−O distance of enediol, as compared to the distance between the two linking titanium atoms. Therefore, caution should be exercised when using this as the most stable structure. There may be another surface where the Ti−Ti distance is optimal for binding quinol without significant structural distortions. The computed FMO energy differences are 1.69 eV (see Figure 3c). These calculated results qualitatively suggest that the delocalization of the electron cloud increases as we move from catechol to

dx.doi.org/10.1021/jp207054f |J. Phys. Chem. C 2012, 116, 98–103

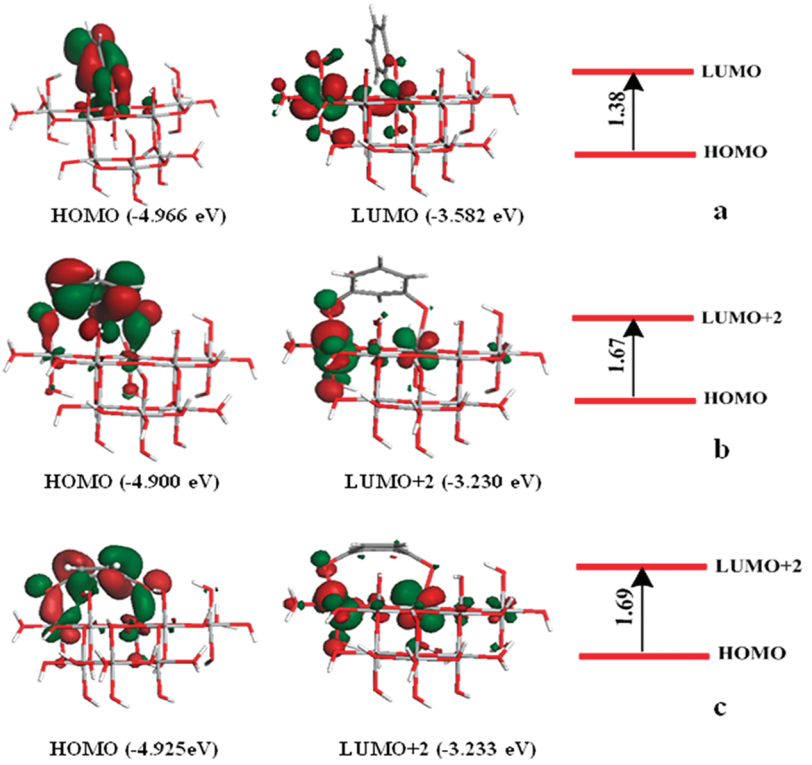

Figure 3. Molecular orbitals for the bound dye to the TiO_2 surface and their corresponding energy differences in eV calculated with GGA/PW91/DND in a chloroform solvent using the COSMO solvation model. (a) Catechol-TiO_2, (b) resorcinol-TiO_2, and (c) quinol-TiO_2.

quinol. This inference is very important from the point of view of charge separation as demonstrated previously by Duncan et al.[10] and Luis et al.[35] for the catechol-TiO_2 system. Their results suggested that the initial localization of the charge on the electron injection is on the Ti attached to the adsorbate. Furthermore, at longer times, the injected electron diffuses along different directions in TiO_2. The diffusion event is anisoptropic due to different electronic dispersions in different directions and is clearly influenced by the delocalization in the initial injection site. By comparing the results from the present study to the previous reports, we find that there is a greater delocalization of charge in the LUMO as we increase the distance between the bridge linkers (catechol to quinol). This greater delocalization, we believe, will help in a better charge diffusion into the bulk of TiO_2. We have also carried out the excited state calculations for all the three dyes complexed with the TiO_2 surface using the ZINDO semiempirical method with configuration interaction (CI). [34,39] The frontier molecular orbitals obtained from ZINDO calculations for catechol, resorcinol, and quinol showed qualitatively a similar trend as obtained from the GGA/PW91/DND level of theory (Figure S2, Supporting Information).

To find out the effect of the binding position in an enediol-TiO_2 system in interfacial ET dynamics and also to find out the contribution between the localized vs delocalized electron transfer reaction, we have carried out femtosecond transient absorption studies. Figure 4 shows the femtosecond transient absorption spectra at different time delays of the resorcinol-TiO_2 and quinol-TiO_2 systems after exciting the samples at 400 nm. The transient spectra show a broad absorption band in the 500−700 nm region and beyond and bleach below 500 nm. The broad positive absorption feature can be assigned to injected CB electrons or to excited state absorptions (ESA) based on previous studies on

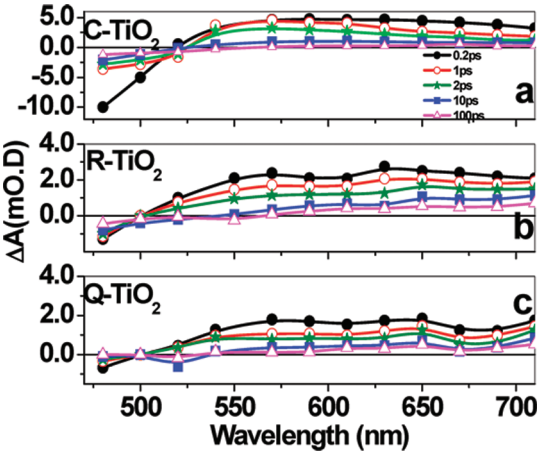

Figure 4. Femtosecond transient absorption spectra of (a) catechol-sensitized TiO_2 nanoparticles, (b) resorcinol-sensitized TiO_2 nanoparticles, and (c) quinol-sensitized TiO_2 nanoparticles in chloroform at different delay times after a 400 nm excitation.

the catechol-TiO_2 system.[16,20] In our earlier investigation,[16] we have reported transient absorption spectra of the catechol-TiO_2 system in environments like water and microemulsion. We have observed a peak at ~600 nm in the transient absorption spectra; however, we could not attribute it to the cation radical peak of catechol, as E.J. Land[36] reported transient spectra of the cation radical of catechol absorbs below 500 nm. It is also possible that the feature at 600 nm might come from the cation radical of catechol; however, it is difficult to assign, as a pulse radiolysis study on catechol clearly shows that the cationic form is not very

dx.doi.org/10.1021/jp207054f |J. Phys. Chem. C 2012, 116, 98–103

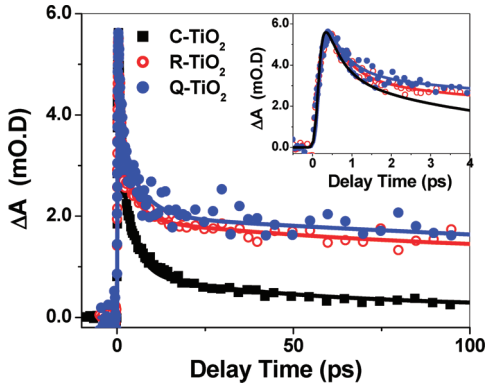

Figure 5. Kinetics traces at 620 nm for different enediol-sensitized TiO_2 nanoparticles in chloroform. Inset: the same kinetics at a shorter time scale.

Table 2. Life Times of the Transients in Enediol-Sensitized TiO_2 Systems after Excitation with a 400 nm (fwhm < 100 fs) Laser Pulse and Monitoring at 620 nm

system/fitting parameters	C-TiO_2	R-TiO_2	Q-TiO_2
τ_1	0.4 ps (63%)	0.4 ps (57%)	0.6 ps (53.8%)
τ_2	3.5 ps (33%)	4 ps (19.8%)	6 ps (20%)
τ_3	>200 ps (4%)	>200 ps (23.2%)	>200 ps (26.2%)

stable at longer time scales. Lian and co-workers[20] also observed a similar transient band in the catechol-TiO_2 system, and they have attributed it to the injected electron in the conduction band of TiO_2. However, we also believe that the transient band might be due to the excited absorption band due to the charge separated state of the enediol-TiO_2 system. So, it is possible that in the cases of resorcinol and quinol the positive absorption band at 600 nm might be also due to the mixture of a cation radical and an injected electron.

To find out the temporal dynamics, we have monitored the kinetics at 620 nm to determine forward and backward ET dynamics for all enediol-sensitized TiO_2 systems, and they are shown in Figure 5. In the present investigation, the 400 nm pump primarily excites the CT complex (Figure 2), which enables direct electron injection into the conduction band of TiO_2. The electron injection was found to be pulse-width limited (<50 fs) as monitored from the appearance time of the signal. It is interesting to note that although the ground state coupling between enediols and TiO_2 NPs varies an order of magnitude from catechol to resorcinol and quinol, we have observed the same pulse-width injection time in all systems. It made us to think that although in case of resorcinol- and quinol-sensitized TiO_2 nanoparticles, H_{ab} is smaller as compared to catechol-sensitized TiO_2 and still the direct population of hot states in the conduction band of TiO_2 still takes place in the R-TiO_2 and Q-TiO_2 systems. Now, to find out the effect of the molecular structure of enediols on the back ET dynamics, we have compared the kinetics and fittings parameters, as shown in Table 2. By comparing the dynamics of the C-TiO_2 system with those of the R-TiO_2 and Q-TiO_2 systems, it clearly indicates that recombination dynamics (back ET) of the R-TiO_2 and Q-TiO_2 systems is considerably slower. It is clearly seen that at the early time scale (<2 ps), BET dynamics follow each other in all three enediol-TiO_2 systems, and later, it deviates. The early time constants can be fitted to 400 fs, which can be attributed to recombination dynamics due to the hot injected electron and parent enediol cation, which also can be attributed to the charge recombination of the localized electron in TiO_2 and the parent cation. It is interesting to see that the recombination dynamics is much faster for C-TiO_2 as compared to the R-TiO_2 and Q-TiO_2 systems. In addition to the fast component, the decay traces are fitted with two longer components (3 and 200 ps), which can be attributed to the charge recombination of the partially delocalized electron in TiO_2 and the parent cation. Our investigation gives clear evidence of the charge delocalization in resorcinol and quinol as compared to that of catechol. Earlier, Lian and co-workers[20] demonstrated ET dynamics in $(NH_4)_2$-$Ti(Cat)_3$ and show that at least 90% of the recombination reaction takes place with the time constant of 0.4 ps. The fast recombination in the above molecular case where delocalization is not present was attributed to strong coupling. As compared to the molecular system as reported by Lian and co-workers,[20] the recombination dynamics in the C-TiO_2 system in the present study is slower, which indicate some degree of delocalization of injected electrons. This point was noted previously by Lian et al.,[18] and the dynamics was explained on the basis of the delocalization of the electron over several Ti centers as compared to the molecular complex. Our study clearly proves that just by varying the position of the OH group in enediols, it is possible to delocalize the electron in TiO_2 and eventually slow down the recombination reaction. The fastest component in the BET dynamics, i.e., ~0.4−0.6 ps present in all of the enediol-TiO_2 systems, arises from a geminate recombination from the initial injection site by hot electron recombination with the HOMO of catechol.[9] We find that the rate of charge recombination reaction decreases from catechol to quinol, indicating that delocalization differs as the distances between the bridge linkers increases (Table 2). The general trend in the slow recombination dynamics as distances between bridging ligands increase indicates the delocalization of the electron is much pronounced in the case of quinol. The BET rate for the enediol-TiO_2 systems in the present investigation can be analyzed in terms of the Marcus theory, which can be expressed in terms of electronic coupling and energetic as follows:[37,38]

$$k_{BET} = \left(\frac{2\pi}{\hbar}\right)[H_{ab}]^2 \frac{1}{\sqrt{4\pi\lambda kT}} \exp\left\{-\frac{(\Delta G^0 + \lambda)^2}{4\lambda kT}\right\}$$

We have calculated $-\Delta G^0$ and λ for all of the enediol-TiO_2 systems, and the calculations are shown in the Supporting Information. As the charge recombination reaction in a dye-TiO_2 system falls in the Marcus inverted regime, the increasing of the free energy of the back ET reaction should slow down if the coupling and other parameters are same. We have observed that λ for catechol (λ = 0.18) and quinol (λ = 0.17) are very similar (see Supporting Information), and the free energy (ΔG^0) for the C-TiO_2 system is determined to be −1.03 eV, and for the Q-TiO2 system, it is −0.96 eV. According to the Marcus theory, the recombination reaction for the C-TiO_2 system should be slower; however, we observed that it is much faster as compared to that of the Q-TiO_2 system. The recombination dynamics shows that in enediol-TiO_2 systems, the prediction of the ET rate does not follow on the basis of free energy alone, which seem to indicate that the electronic coupling seems to play a major role in the recombination dynamics.

4. CONCLUSIONS

In conclusion, our study clearly indicates that as we increase the distance between two OH groups in enediol, the rate of charge recombination decreases due to delocalization of the injected electron in TiO_2. This observation is important from the point of view of application as we prove in the present study that we can control the electronic coupling by just varying the position of the bridge linkers. Studies on the control of electron transfers had earlier exploited the effect of orientation between the donor and acceptor, variation in binding groups, etc. Here, we show that control of electron transfer can also be achieved by varying just the bridge linkers without any change in the binding group involved.

■ ASSOCIATED CONTENT

Supporting Information. Details about the BH plot; calculation of free energy for the BET process; and the computational methodology. This material is available free of charge via the Internet at http://pubs.acs.org.

■ AUTHOR INFORMATION

Corresponding Author

*E-mail: hnghosh@barc.gov.in (H.N.G); ganguly@csmcri.org (B.G.).
§E-mail: sreeji@barc.gov.in (S.K.).

■ ACKNOWLEDGMENT

We thank Dr. D.K. Palit, Dr. S.K. Sarkar, and Dr. T. Mukherjee for their encouragement and continuous support. A.S. is thankful to UGC, New Delhi, India for the awarding of the senior research fellowship. We thank the reviewers for their comments/suggestions that have helped us to improve this article.

■ REFERENCES

(1) (a) Miller, R. J. D.; McLendon, G. L.; Nozik, A. J.; Schmickler, W.; Willig, F. *Surface Electron-Transfer Processes*; VCH Publishers, Inc.: New York, 1995.
(2) Kamat, P. V.; Meisel, D. Semiconductor Nanoclusters Physical. In *Chemical & Catalytic Aspects*; Elsevier: Amsterdam, The Netherlands, 1997; Vol. 103.
(3) Graetzel, M. *Acc. Chem. Res.* **1981**, *148*, 376–384.
(4) Linsebigler, A. L.; Lu, G. Q.; Yates, J. T. *Chem. Rev.* **1995**, *95*, 735.
(5) O Regan, B.; Gratzel, M. *Nature* **1991**, *353*, 737.
(6) Alivisatos, A. P. *J. Phys. Chem.* **1996**, *100*, 13226.
(7) Piotrowiak, P.; Galoppini, E. W. Q.; Meyer, G. J.; Wiewior, P. *J. Am. Chem. Soc.* **2003**, *125*, 5278.
(8) She, C.; Anderson, N. A.; Guo, J.; Liu, F.; Goh, W.-H.; Chen, D.-T.; Mohler, D. L.; Tian, Z.-Q.; Hupp, J. T.; Lian, T. *J. Phys. Chem. B* **2005**, *109*, 19345.
(9) Gundlach, L.; Ernstorfer, R.; Willig, F. *Phys. Rev. B* **2006**, *74*, 035324.
(10) Duncan, W. R.; Prezhdo, O. V. *Annu. Rev. Phys. Chem.* **2007**, *58*, 143.
(11) Ramakrishna, G.; Ghosh, H. N.; Singh, A. K.; Palit, D. K.; Mittal, J. P. *J. Phys. Chem. B* **2001**, *105*, 12786.
(12) Schnadt, J.; Brühwiler, P. A.; Patthey, L.; O'Shea, J. N.; Södergren, S.; Odelius, M.; Ahuja, R.; Karis, O.; Bässler, M.; Persson, P.; Siegbahn, H.; Lunell, S.; Mårtensson, N. *Nature* **2002**, *418*, 620.
(13) Matylitsky, V. V.; Lenz, M. O.; Wachtveitl, J. *J. Phys. Chem. B* **2006**, *110*, 8372.
(14) Ramakrishna, G.; Singh, A. K.; Palit, D. K.; Ghosh, H. N. *J. Phys. Chem. B* **2004**, *108*, 1701.
(15) Steenken, S.; Neta, P. *J. Phys. Chem.* **1982**, *86*, 3661.
(16) Rath, M. C.; Palit, D. K.; Mukherjee, T.; Ghosh, H. N. *J. Photochem. Photobiol., A* **2009**, *204*, 209.
(17) Sreejith, K.; Rawalekar, S.; Verma, S.; Ghosh, H. N. *Phys. Chem. Chem. Phys.* **2010**, *12*, 4210.
(18) Wang, P.; Xie, T.; Peng, L.; Li, H.; Wu, T.; Pang, S.; Wang, D. *J. Phys. Chem. C* **2008**, *112* (17), 6648–6652.
(19) Duncan, W. R.; Prezhdo, O. V. *J. Phys. Chem. B* **2005**, *109*, 365.
(20) Wang, Y.; Hang, K.; Anderson, N. A.; Lian, T. *J. Phys. Chem. B* **2003**, *107*, 9434.
(21) Mulliken, R. S. *J. Am. Chem. Soc.* **1952**, *64*, 811.
(22) Hush, N. S. *Prog. Inorg. Chem.* **1967**, *8*, 391.
(23) *Materials Studio* DMOL3, version 4.1; Accelrys Inc.: San Diego, CA.
(24) Perdew, J. P.; Wang, Y. *Phys. Rev. B* **1992**, *45*, 13244.
(25) Wu, Z.; Cohen, R. E.; Singh, D. *J. Phys. Rev. B* **2004**, *70*, 104112.
(26) Ziesche, P.; Kurth, S.; Perdew, J. P. *Comput. Mater. Sci.* **1998**, *11*, 122.
(27) Kohn, W.; Becke, A. D.; Parr, R. G. *J. Phys. Chem.* **1996**, *100*, 12974.
(28) Perdew, J. P.; Burke, K.; Ernzerhof, M. *Phys. Rev. Lett.* **1996**, *77*, 3865.
(29) Chiodo, L.; García-Lastra, J. M.; Iacomino, A.; Ossicini, S.; Zhao, J.; Petek, H.; Rubio, A. *Phys. Rev. B* **2010**, *82*, 045207.
(30) Prezhdo, O. V.; Duncan, W. R.; Prezhdo, V. V. *Prog. Surf. Sci.* **2009**, *84*, 30.
(31) Klamt, A. COSMO and COSMO-RS. In *Encyclopedia of Computational Chemistry*; von Rague Schleyer, P., Allinger, N. L., Eds.; Wiley: New York, 1998; Vol. 2, p 604.
(32) Klamt, A. *J. Phys. Chem.* **1995**, *99*, 2224–2235.
(33) Klamt, A.; Jonas, V.; Bürger, T.; Lohrenz, J. C.W. *J. Phys. Chem. A* **1998**, *102*, 5074–5084.
(34) Redfern, P. C.; Zapol, P.; Curtiss, L. A.; Rajh, T.; Thurnauer, M. C. *J. Phys. Chem. B* **2003**, *107*, 11419.
(35) Rego, L. G. C.; Batista, V. S. *J. Am. Chem. Soc.* **2003**, *125*, 7989.
(36) Land, E. J. *J. Chem. Soc., Faraday Trans.* **1993**, *89*, 803.
(37) Marcus, R. A. *Annu. Rev. Phys. Chem.* **1964**, *15*, 155.
(38) Marcus, R. A.; Sutin, N. *Biochim. Biophys. Acta* **1985**, *811*, 265.
(39) Nogueira, A. F.; Fernando, L.; Furtado, O.; Formiga, A. L. B.; Nakamura, M.; Araki, K.; Toma, H. E. *Inorg. Chem.* **2004**, *43*, 396–398.